© 2015. Published by The Company of Biologists Ltd | Development (2015) 142, 3675-3685 doi:10.1242/dev.125708

RESEARCH ARTICLE

STEM CELLS AND REGENERATION

Differential DNA damage signalling and apoptotic threshold correlate with mouse epiblast-specific hypersensitivity to radiation

Audrey Laurent* and Francesco Blasi*

ABSTRACT

Between implantation and gastrulation, mouse pluripotent epiblast cells expand enormously in number and exhibit a remarkable hypersensitivity to DNA damage. Upon low-dose irradiation, they undergo mitotic arrest followed by p53-dependent apoptosis, whereas the other cell types simply arrest. This protective mechanism, active exclusively after E5.5 and lost during gastrulation, ensures the elimination of every mutated cell before its clonal expansion and is therefore expected to greatly increase fitness. We show that the insurgence of apoptosis relies on the epiblast-specific convergence of both increased DNA damage signalling and stronger pro-apoptotic balance. Although upstream Atm/Atr global activity and specific γH2AX phosphorylation are similar in all cell types of the embryo, 53BP1 recruitment at DNA breaks is immediately amplified only in epiblast cells after ionizing radiation. This correlates with rapid epiblast-specific activation of p53 and its transcriptional properties. Moreover, between E5.5 and E6.5 epiblast cells lower their apoptotic threshold by enhancing the expression of pro-apoptotic Bak and Bim and repressing the anti-apoptotic Bcl-xL. Thus, even after low-dose irradiation, the cytoplasmic priming of epiblast cells allows p53 to rapidly induce apoptosis via a partially transcription-independent mechanism.

KEY WORDS: Epiblast, Apoptosis, DNA damage response, Trp53bp1, Cytoplasmic apoptotic priming

INTRODUCTION

Maintenance of genomic integrity is important in stem cells for tissue differentiation and homeostasis (Blanpain et al., 2011). It is particularly crucial in the epiblast (Epi), which undergoes a major expansion and has the potential to contribute to all tissues, including the germline. Acquisition of post-zygotic mutations during embryonic development may alter organogenesis or favour tumour formation later in life (Greaves and Wiemels, 2003; Hafner et al., 2011; Marshall et al., 2014; Mori et al., 2002). In spite of their major importance, cell growth regulation and DNA damage response during embryogenesis remain poorly understood.

One stage of the early mouse development is particularly important. As the embryo implants, it is composed of extra-embryonic annexes and a restricted pool of slowly dividing pluripotent cells, the Epi, from which the embryo proper will originate (Takaoka and Hamada, 2012). Soon after implantation at embryonic day (E) 4, the Epi enters a phase of intense proliferation in order to produce the cells necessary for gastrulation, which initiates at E7.0 (Solter et al., 1971; Stuckey et al., 2011). From 120 cells composing the Epi of an E5.5 post-implantation embryo, it is estimated that about 14,500 cells are generated by the end of the gastrulation (Snow, 1977). Thus, at E6.5-7.5 the Epi cells are dividing very actively and might therefore be particularly prone to accumulate mutations, which would be detrimental for further development. In fact, the post-implantation growth of the Epi corresponds to a very sensitive developmental window during which the deletion of several genes instrumental for genome integrity is lethal (Brown and Baltimore, 2000; Dobles et al., 2000; Hakem et al., 1996; Jeon et al., 2011; Kalitsis et al., 2000). Remarkably, it has been reported that during this phase the mouse embryo is hypersensitive to DNA damage and undergoes apoptosis without cell cycle arrest when irradiated even with low doses (Heyer et al., 2000). This protective mechanism, eliminating every potentially dangerous mutation carrier before its clonal expansion, is expected to greatly enhance organism fitness.

Upon induction of DNA double-stranded breaks, the DNA damage response is initiated on the local chromatin, then spreads into adjacent sites and is amplified, ultimately leading to the activation of effector proteins, such as p53 (Trp53) (Panier and Boulton, 2014). Depending on the cell context, the activation of p53 triggers arrest, repair, differentiation, senescence or apoptosis (Carvajal and Manfredi, 2013). Several studies performed in human embryonic stem cells (ESCs) or mouse peri-gastrulation embryos revealed that various mechanisms may prime stem cells for apoptosis, such as the presence of constitutively active Bax at the Golgi (Dumitru et al., 2012), an imbalance between pro- and anti-apoptotic factors lowering the apoptotic threshold (Liu et al., 2013), or the control of Bim (Bcl2l11) expression by miRNAs, which would allow a fast release upon stress induction (Pernaute et al., 2014).

Here, we characterise in peri-gastrulation mouse embryos the cell type heterogeneity of the radiation-induced DNA damage response. After E5.5, although all cell types undergo mitotic arrest upon exposure to ionizing radiation, only the Epi cells and their primitive streak (PrS) progeny exhibit an apoptotic response. We show the Epi-specific convergence of an amplified DNA damage signalling at the level of 53BP1 (Trp53bp1) recruitment, resulting in rapid and specific activation of p53, and a cytoplasmic priming due to increased Bak (Bak1) and Bim and decreased Bcl-xL (Bcl2l1) expression, causing DNA damage-induced cell death.

RESULTS

The Epi of peri-gastrulation embryos is highly proliferative and shows replicative stress

First, we measured the mitotic index (MI) of the Epi, visceral endoderm (VE) and extra-embryonic ectoderm (ExE) at E6.5 and E7.5, using Ser10-phosphorylated histone H3 (P-H3) as a mitotic marker (Hendzel et al., 1997) and Oct4 (Pou5f1) (Palmieri et al., 1994) and brachyury (T) (Herrmann et al., 1990) as specific markers

IFOM (FIRC Institute of Molecular Oncology), IFOM-IEO-Campus, Via Adamello 16, 20139 Milan, Italy.

*Authors for correspondence (la.audrey@outlook.fr; francesco.blasi@ifom.eu)

Received 27 April 2015; Accepted 8 September 2015

Development (2015) 142, 3675-3685 doi:10.1242/dev.125708

of the Epi at E6.5 and of the PrS derivatives at E7.5, respectively. For each cell type, the MI was calculated as the percentage of P-H3$^+$ among DAPI$^+$ cells. At both E6.5 and E7.5, the MI of the Epi was significantly higher than that of extra-embryonic tissues. At E6.5, we measured an MI of 13.2% in the Epi versus 5% and 2% in the ExE and VE, respectively (Fig. S1A), and at E7.5 an MI of 10.7% versus 4% and 5.5% in the ExE and the VE (Fig. S1B). At E7.5, among the brachyury$^+$ cells, those localised in the embryonic region had an MI of 6.5%, whereas those in the extra-embryonic mesoderm territories had an MI of 3.5% (Fig. S1B). This confirms that at peri-gastrulation stage the whole embryo is expanding consistently in both embryonic and extra-embryonic compartments, but the Epi and the embryonic PrS are the fastest dividing tissues.

Rapid cell cycles may induce replicative stress, stalling and collapse of replication forks or interference between transcription and replication machineries (Zeman and Cimprich, 2014). The phosphorylated form of histone H2AX (γH2AX), which has mostly been used to detect DNA damage foci at double-stranded breaks (i.e. after irradiation), is however also accumulated on chromatin under replicative stress. Therefore, γH2AX may be used as a marker of replicative stress in rapidly dividing cells, such as cancer cells (Seo et al., 2012; Ward and Chen, 2001). In untreated E6.5 embryos we detected endogenous γH2AX both in the Epi and in the ExE, suggesting that these tissues are dealing with replicative stress (Fig. S1C). By contrast, VE cells, with a lower MI, appeared negative for this marker. The basal phosphorylation of H2AX observed in the Epi and ExE, however, does not correlate with the formation of 53BP1 foci (Fig. S1D), which is a documented marker of DNA damage (Anderson et al., 2001). This result supports the hypothesis that, in early embryos, detection of γH2AX is linked to replicative stress and not to the activation of the DNA damage response pathway.

At E6.5 ionizing radiation induces general mitotic arrest and Epi-specific apoptosis

To explore the effect of exogenous DNA damage on cell cycle and survival, E6.5 embryos were X-ray irradiated with 5 Gy and cultured for 10 min to 2 h before fixation and immunostaining. In contrast to a previous report (Heyer et al., 2000), the MI of treated embryos was decreased to 2.7% 30 min after irradiation and to 0.3% after 1 h, whereas non-irradiated samples had an MI of 9.5% (Fig. 1A). The mitotic arrest was observed in both Epi and extra-embryonic tissues, suggesting that at E6.5 all cells have active cell cycle checkpoints, including the rapidly cycling Epi cells.

In addition, irradiation quickly induced apoptosis in the embryos, as evidenced by cleaved caspase 3 (Cl Casp-3) staining (Fig. 1B). Indeed, the apoptotic index of the embryos drastically increased from 1-2.5% in non-irradiated controls to 15.5% 1.5 h after 5 Gy irradiation and to 29% after 2 h. Using a substantially lower radiation dose of 0.5 Gy, we measured apoptotic indexes of 10.2% and 16.7% at 1.5 and 2 h, respectively, after exposure to radiation (Fig. 1B). Finally, caspase 3 cleavage after irradiation was associated with Bax activation (Fig. 2A), indicating that the DNA damage-induced apoptosis observed in the E6.5 embryos is driven by the mitochondrial pathway, in agreement with reports in other cell types (Hsu et al., 1997).

Radiation hypersensitivity of peri-gastrulation embryos is cell type and stage specific

The DNA damage-induced apoptosis was cell type specific. Indeed, 2 h after exposure to 0.5 Gy ionizing radiation (Fig. 2A), or 1.5 h after 5 Gy (Fig. S2), only the Epi cells stained positively for Cl Casp-3 and active Bax. Therefore, Epi cells are more sensitive than the adjacent ExE and VE cells to the same physical stress.

We then investigated whether the specific sensitivity of the Epi to irradiation can be observed at an earlier developmental stage or is acquired during its maturation. In E5.5 embryos, irradiation with 0.5 Gy did not trigger apoptosis (Fig. 2B, upper panels), but it induced a general mitotic arrest (Fig. 2B, lower panels). Indeed, P-H3 staining was completely negative in treated embryos, whereas controls showed an MI of 7.6%. We conclude that DNA damage signalling occurs in E5.5 embryos, which respond with a mitotic arrest. However, at this stage Epi cells are resistant to apoptosis.

Conversely, in the gastrulating E7.5 embryo, the PrS-derived cells, which originate from the Epi but are committed toward differentiation, showed two types of behaviour upon exposure to 0.5 Gy radiation. Among the brachyury$^+$ population located in the embryonic area (the mesendoderm progenitors), posterior cells underwent massive apoptosis (red arrow), whereas those which had reached the anteriormost region of the embryo were clearly Cl Casp-3$^-$ (green arrow) (Fig. 2C). The cells contributing to the extra-embryonic mesoderm were also Cl Casp-3$^-$. This suggests that cells lose their hypersensitivity as they migrate away from the PrS and differentiate. As in E6.5 embryos, ExE and VE cells did not show hypersensitivity, whereas Epi cells underwent massive apoptosis.

Altogether, our data argue that at E6.5-7.5 the Epi and PrS are hyperproliferative and hypersensitive to DNA damage. To elucidate the molecular basis of this differential response to irradiation, we studied the DNA damage response cascade in E6.5 embryos, which leads to Epi-specific Bax activation and caspase 3 cleavage.

The Atm/Atr pathway is equally active in the Epi, VE and ExE upon irradiation

Upon DNA damage, the major upstream kinases Atm and Atr phosphorylate a large number of substrates at an S/TQ consensus sequence (Kim et al., 1999). In E6.5 embryos, immunofluorescence using an anti-phosphorylated S/TQ motif (P-S/TQ) antibody showed similar staining in the Epi, VE and ExE after exposure to 0.5 Gy radiation (Fig. 3A). The same result was observed upon a 10-fold higher irradiation dose (5 Gy) (Fig. S3A). These results suggest that the Atm/Atr pathway is equally active in all three tissues of the embryo. Of note, the signal observed in the non-irradiated control embryos corresponds to a staining of the mitotic chromosomes in the Epi cells, independent of exogenous DNA damage (see the control staining in Fig. S3B).

In addition, among Atm/Atr targets, H2AX is rapidly phosphorylated at the double-stranded breaks and typical γH2AX foci can be detected. Similar to P-S/TQ, 10 min after 0.5 Gy irradiation, γH2AX foci formation was comparable in Epi and extra-embryonic cells (Fig. 3B). Quantification of the amount of fluorescence per cell showed no significant difference between cell types. Therefore, no difference in the activity of Atm/Atr between Epi and extra-embryonic cells was detectable when testing P-S/TQ motifs or when investigating the specific phosphorylation of H2AX.

Finally, although Atm is considered as the kinase of choice in the response to double-stranded breaks, it was not essential to radiation-induced apoptosis. Indeed, we observed a strong Cl Casp-3 signal in *Atm*-null embryos after 0.5 Gy irradiation (Fig. 3C). In contrast to a previous report (Heyer et al., 2000), our result agrees with the majority of the literature in that Atm deficiency sensitises cells to DNA damage (Williamson et al., 2010). Since very few cells remained in the Epi of *Atm*-null embryos 2 h after irradiation, the TUNEL analysis presented by Heyer et al. (2000) might not have

Development (2015) 142, 3675-3685 doi:10.1242/dev.125708

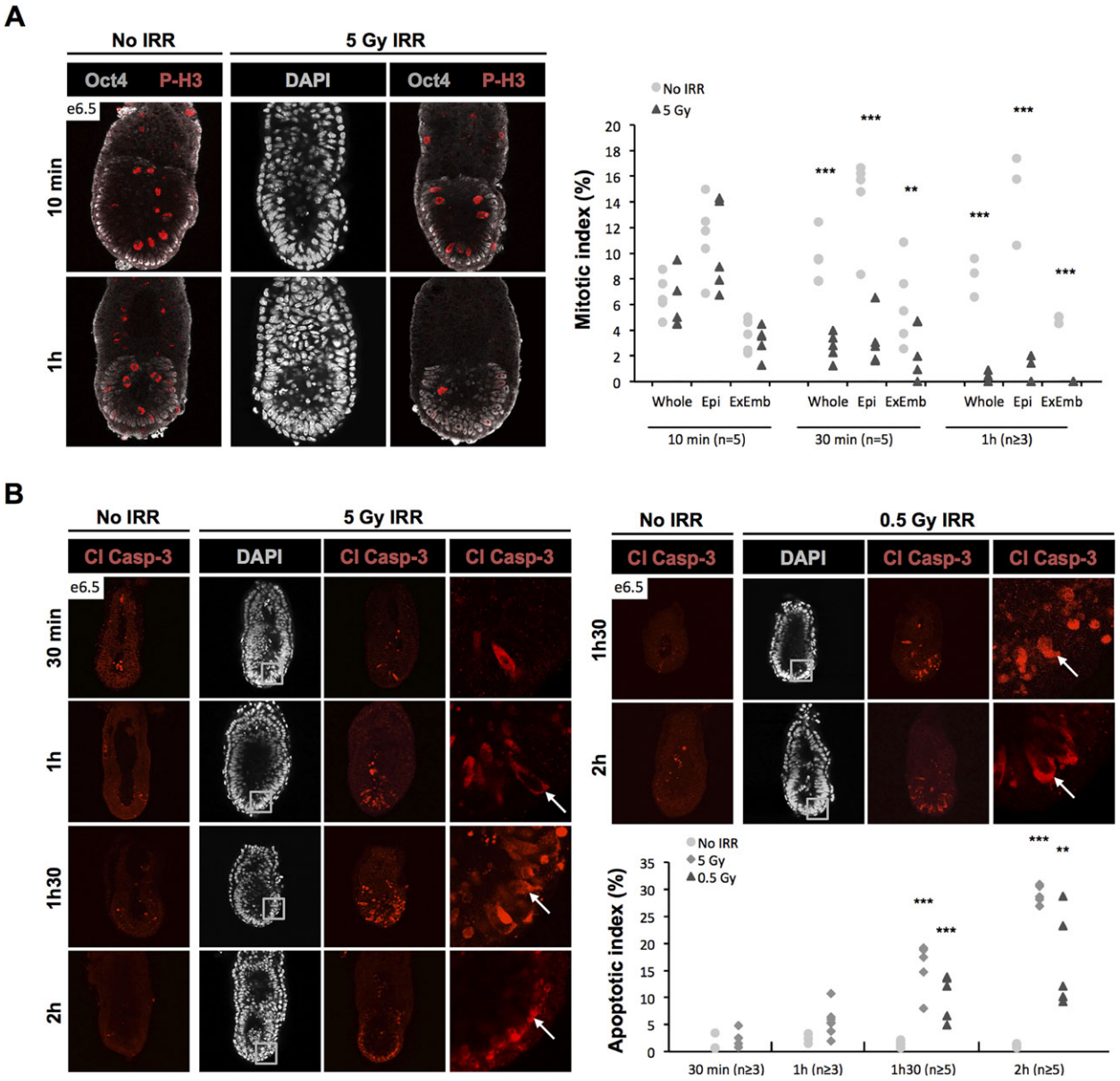

Fig. 1. Irradiation of E6.5 mouse embryos induces cell cycle arrest and apoptosis. (A) Representative immunostaining of P-H3 and Oct4 in E6.5 embryos 10 min and 1 h after 5 Gy irradiation (IRR) and in controls (no IRR). To the right is plotted the quantification of mitotic index (MI) found in each condition at 10 min. *n*=5 for each condition and time point, except 1 h: no IRR, *n*=4; 5 Gy, *n*=3. (B) (Left) Representative immunostaining of Cl Casp-3 in E6.5 embryos 30 min (*n*=4), 1 h (*n*=8), 1.5 h (*n*=6) and 2 h (*n*=5) after 5 Gy irradiation; for no IRR controls: 30 min and 1 h, *n*=3; 1.5 h and 2 h, *n*=5. (Right) Representative immunostaining of Cl Casp-3, 1.5 h (*n*=5) and 2 h (*n*=6) after 0.5 Gy irradiation in E6.5 embryos and controls. Boxed regions are shown magnified 5-fold in the fourth columns. Arrows indicate apoptotic cells. The apoptotic indexes measured in each condition are represented in the plot. Embryos were counterstained with DAPI. ***P<0.005 and **P<0.05, Student's *t*-test.

detected them. We conclude that radiation-induced apoptosis in the Epi does not strictly depend on Atm, which may be compensated by Atr and/or DNA-PK kinases (Callén et al., 2009; Gurley and Kemp, 2001; Siliciano et al., 1997).

53BP1 focal recruitment at double-stranded breaks is amplified in the Epi

In the absence of any differential activation of upstream DNA damage signalling, we then analysed 53BP1, which acts downstream of Atm/Atr and H2AX phosphorylation. 53BP1 is essential for the activation of the effectors Chk2 (Chek2) and p53 (Wang et al., 2002; Ward et al., 2003). Widely expressed in the nucleus under normal conditions, 53BP1 is recruited at the DNA damage foci upon irradiation. Remarkably, 10 min after 0.5 Gy irradiation, typical 53BP1 foci were clearly detectable in the Epi (Fig. 3D), but not in VE and ExE cells, where the staining was more diffuse and the foci weaker and smaller. Quantitation of the amount of fluorescence per cell revealed a 3.5-fold stronger response in Epi cells versus extra-embryonic tissues. This difference persisted over time, as the same observation was made 30 min and 1 h after irradiation (Fig. S4A). A similar result was obtained 30 min after a 10-fold higher radiation dose (Fig. S4B). Since the 53BP1 basal level is the same in the Epi, VE and ExE, its higher focal recruitment in Epi cells cannot be due to enhanced expression (Fig. S1D). Therefore, the Epi, ExE and VE cells present different signalling activities at the site of DNA lesions, since in Epi cells γH2AX-positive foci are more efficient in recruiting 53BP1.

Development (2015) 142, 3675-3685 doi:10.1242/dev.125708

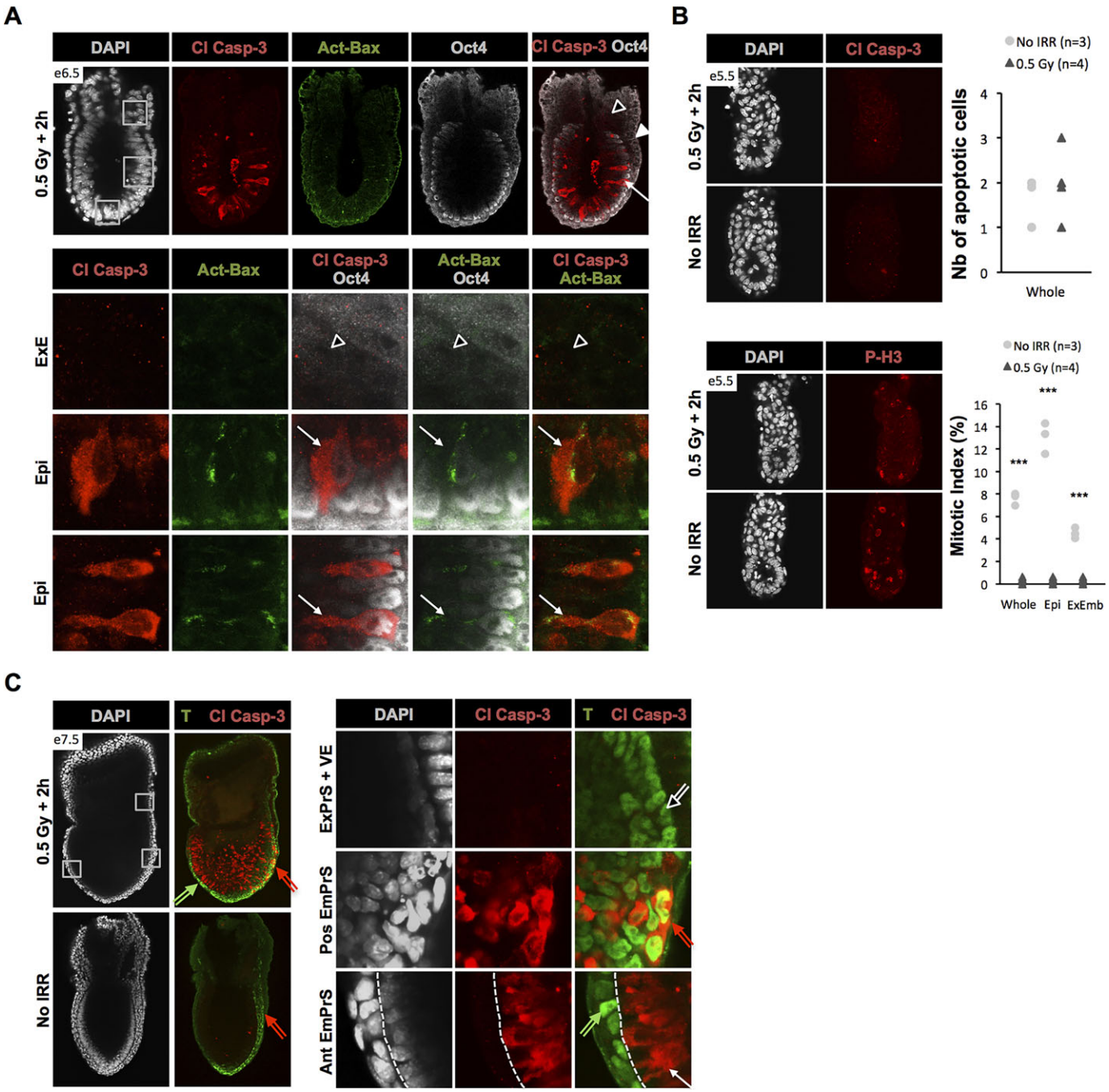

Fig. 2. Radiation hypersensitivity of peri-gastrulation embryos is tissue and stage specific. (A) Representative immunostaining of Cl Casp-3, activated (Act) Bax and Oct4 in an E6.5 embryo 2 h after 0.5 Gy irradiation (*n*=6). Boxed regions are shown magnified beneath. (B) Representative immunostaining of Cl Casp-3 (top) and P-H3 (bottom) in E5.5 embryos 2 h after 0.5 Gy irradiation (*n*=4) and in controls (*n*=3). Plots show the number of apoptotic cells and the MI quantified in each condition in whole embryos (Whole), Epi, or extra-embryonic tissues (ExEmb). ***P<0.005, Student's *t*-test. (C) Representative immunostaining of Cl Casp-3 and brachyury (T) in an E7.5 embryo 2 h after 0.5 Gy irradiation (*n*=5) and in control (*n*=5). Boxed regions are shown magnified 4-fold to the right. The dashed line marks the border between the Epi and PrS. Embryos were counterstained with DAPI. Arrows, Epi; filled arrowhead, VE; empty arrowheads, ExE; red double arrows, posterior embryonic PrS (PosEmPrS); green double arrows, anterior embryonic PrS (AntEmPrS); empty double arrow, extra-embryonic PrS (ExPrS).

After the appearance of γH2AX-positive foci, several enzymes are required to set up the epigenetic environment responsible for 53BP1 recruitment: Rnf8, Rnf168, Tip60 (Kat5), Hdac1, Hdac2, Nsd1, Nsd2 (Whsc1) and UbcM4 (Ube2l3). To gain insight into the molecular basis of Epi-specific 53BP1 recruitment, we compared the endogenous expression of these genes in the Epi versus extra-embryonic tissues. We dissected non-irradiated embryos at the embryonic/extra-embryonic border, extracted RNA and performed qRT-PCR in the two independent Oct4^{+}-enriched and Oct4^{-}-enriched cell populations, below designated distal and proximal portions, respectively (Fig. S5A-C). For feasibility and ethical needs to restrict the number of embryos, we used E7.5 embryos. *Rnf8*, *Tip60*, *Nsd1*, *Nsd2* and *UbcM4* mRNAs were not differentially expressed (Fig. S5D). However, *Rnf168*, *Hdac1* and *Hdac2* were expressed more strongly in the distal cell population at 1.35-fold, 1.3-fold and 1.4-fold, respectively, values close to our

Development (2015) 142, 3675-3685 doi:10.1242/dev.125708

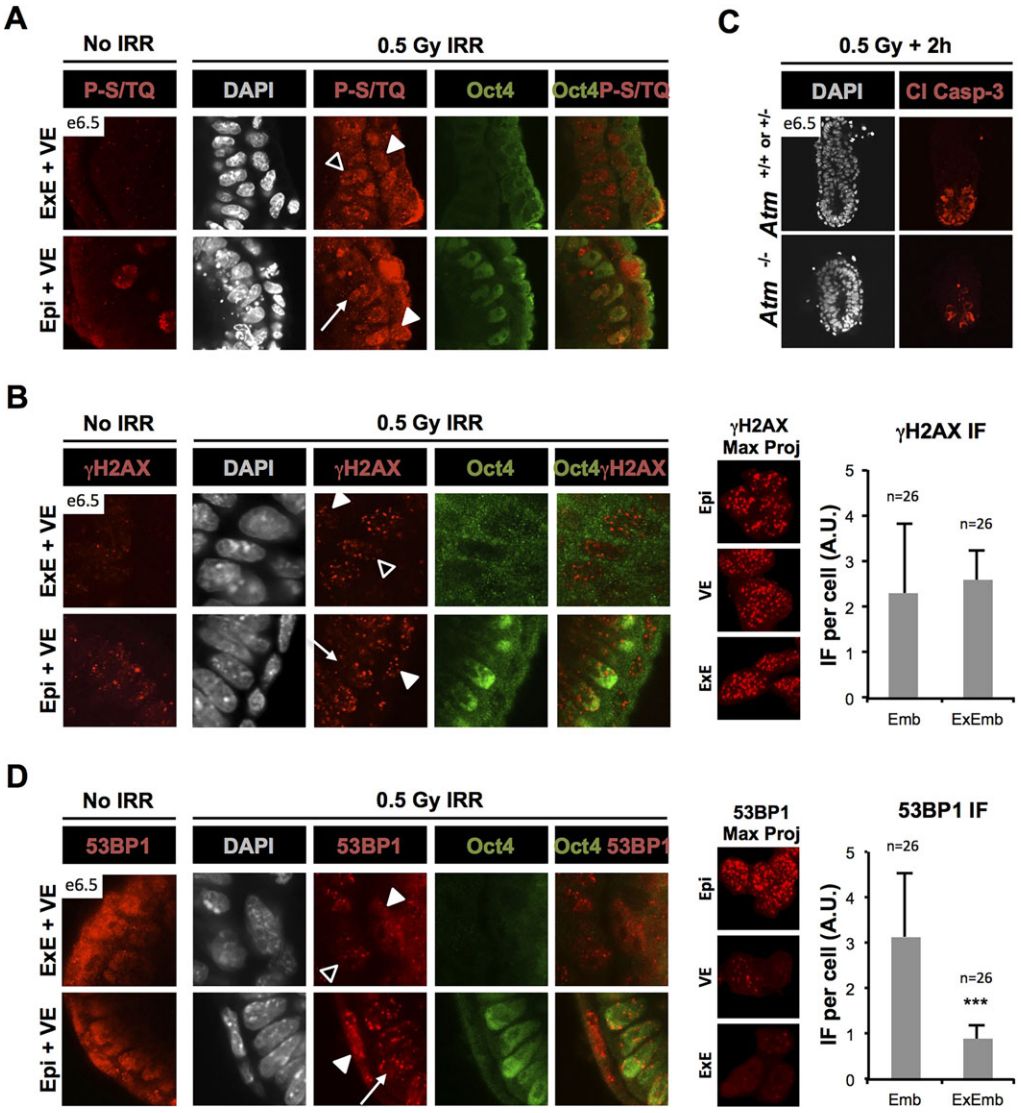

Fig. 3. The DNA damage response is amplified in Epi cells at the level of 53BP1. (A) Representative high-magnification images of P-S/TQ and Oct4 immunostaining in an E6.5 embryo after 0.5 Gy irradiation (n=5) and non-irradiated control (n=5). (B) Representative high-magnification images of γH2AX and Oct4 immunostaining 10 min after 0.5 Gy irradiation in an E6.5 embryo (n=5) and control (n=3). To the right, representative maximum z-projections of γH2AX performed on cropped images are shown. The plot shows the relative amounts of fluorescence (IF) per cell measured in the Epi (Emb) versus extra-embryonic tissues (ExEmb) (26 cells per tissue). (C) Representative immunostaining of Cl Casp-3 and Oct4 in 0.5 Gy irradiated E6.5 WT ($Atm^{+/+ \text{ or } +/-}$; n=7) and $Atm^{-/-}$ (n=2) embryos. (D) Representative high-magnification images of 53BP1 and Oct4 immunostaining 10 min after 0.5 Gy irradiation in an E6.5 embryo (n=6) and control (n=4). To the right, representative maximum z-projections of 53BP1 performed on cropped images are shown. The plot represents the relative amounts of fluorescence per cell measured in the Epi (Emb) versus extra-embryonic tissues (ExEmb) (26 cells per tissue). ***P<0.005, Student's t-test; error bars indicate s.d. Embryos were counterstained with DAPI. Arrows, Epi; filled arrowheads, VE; empty arrowheads, ExE.

personal experience of biological relevance (1.5). Therefore, the high responsiveness of the Epi chromatin to radiation-induced DNA damage might depend on the enhanced expression of these enzymes.

Irradiation induces Epi-specific activation of p53 and its transcriptional properties

p53 is the ultimate coordinator of DNA damage sensing and cell fate decision (Kracikova et al., 2013). The stronger focal recruitment of 53BP1 at the DNA breaks suggests that Epi cells can achieve a greater amplification of DNA damage signalling, resulting in differential activation of its main effector p53. Among the various post-translational modifications of p53, we chose to study the phosphorylation of Ser18 (which corresponds to Ser15 in human P53) because it is central to its activation and triggers a sequential series of additional phosphorylation events in the protein (Carvajal and Manfredi, 2013; Dumaz et al., 1999; Saito et al., 2002; Siliciano et al., 1997).

Remarkably, Ser18-phosphorylated p53 (P-p53) was detected in 100% of Epi cells as early as 10 min after 0.5 Gy irradiation (Fig. 4A), whereas in ExE cells a consistent signal for P-p53 was observed only after 1 h. Even at this time, only a fraction of the VE cells were P-p53^{+}. Irradiation of the embryos with a 10-fold higher dose (5 Gy) led to a similar observation: although now slightly faster, the activation of p53 in the ExE and VE was reproducibly delayed compared with the Epi (Fig. S6A). This result is relevant because the irradiation-induced apoptosis of the Epi is p53 dependent. Indeed, we confirmed previously reported data (Heyer et al., 2000) showing that apoptosis is drastically reduced in *p53*-null embryos 1 h after 5 Gy irradiation (Fig. 4B). We conclude that the hypersensitivity of Epi cells to apoptosis may rely on their unique capacity to rapidly activate p53 upon DNA injury. In addition, immunoreactivity for p53 total protein was equally intense in the ExE, VE and Epi (Fig. S6B), suggesting that the abundant P-p53 found in the Epi is a consequence of the increased DNA damage response (in particular, amplified 53BP1 focal recruitment) and not of elevated endogenous p53 expression.

We then tested whether the rapid phosphorylation of p53 correlated with a transcriptional induction of its target genes. We extracted RNA from 0.5 Gy irradiated E7.5 embryos and performed RT-PCR to assay the expression of p53 targets. Embryos were dissected at the embryonic/extra-embryonic border prior to lysis, as described before (Fig. S5A,B). In the distal cell population (containing the Epi cells), *p21* (*Cdkn1a*) and *Noxa* (*Pmaip1*) genes were respectively induced 2.35-fold and 1.5-fold 1 h after 0.5 Gy irradiation (Fig. 4C), whereas *Bax* and *Mdm2* were not

Development (2015) 142, 3675-3685 doi:10.1242/dev.125708

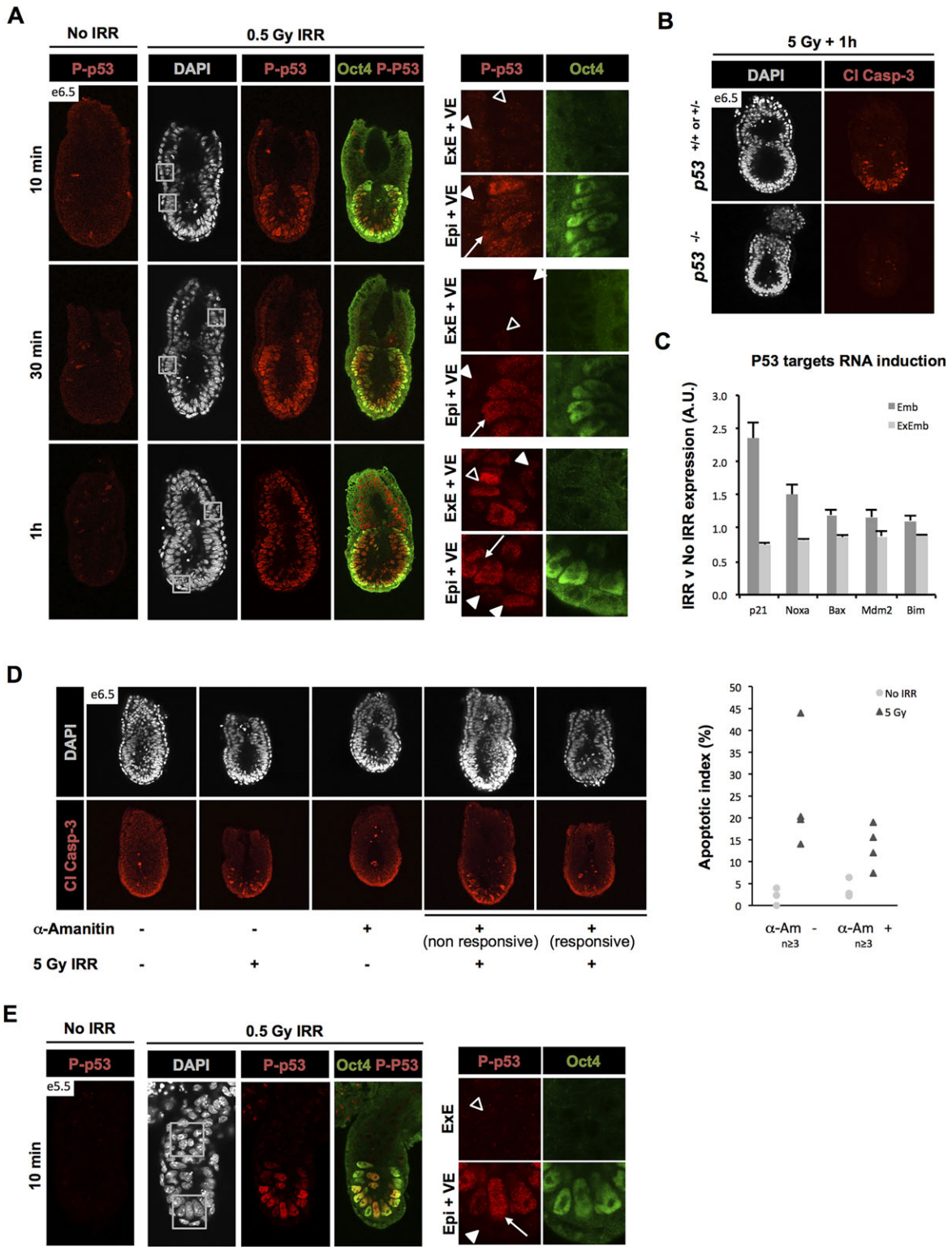

Fig. 4. Rapid activation of p53 in pluripotent Epi cells. (A) Representative images of P-p53 and Oct4 immunostaining in 0.5 Gy irradiated E6.5 embryos and controls (no IRR) 10 (*n*=3 and *n*=4, respectively), 30 (*n*=3 and *n*=5, respectively) or 60 min (*n*=5 for each) after treatment. Boxed regions are shown magnified 5-fold to the right. (B) Representative immunostaining of Cl Casp-3 in 5 Gy irradiated E6.5 WT (*p53*$^{+/+\ or\ +/-}$; *n*=8) and *p53*$^{-/-}$ (*n*=3) embryos. (C) Transcriptional induction of *p21*, *Noxa*, *Bax*, *Mdm2* and *Bim* in E7.5 distal (Emb) and proximal (ExEmb) cell populations, calculated for each tissue as the ratio of expression measured 1 h after 0.5 Gy irradiation versus non-irradiated control (*n*=3); error bars indicate s.d. *P*-values (Student's *t*-test) for Emb and ExEmb, respectively: *p21* RNA, $P=6.72\times10^{-5}$ and $P=1.50\times10^{-4}$; *Noxa* RNA, $P=0.00125$ and $P=1.94\times10^{-4}$; *Bax* RNA, $P=0.00518$ and $P=3.86\times10^{-4}$; *Mdm2* RNA, $P=0.0626$ and $P=0.0722$; *Bim* RNA, $P=0.0434$ and $P=1.018\times10^{-4}$. (D) Representative immunostaining of Cl Casp-3 in 0.5 Gy irradiated E6.5 embryos and controls in the absence or presence of 50 µg/ml α-amanitin. The plot shows the quantification of apoptotic indexes measured in each condition. (E) Representative P-p53 and Oct4 immunostaining 10 min after 0.5 Gy irradiation in E5.5 embryos (*n*=4) and controls (*n*=4). Boxed regions are shown magnified 2.5-fold to the right. Embryos were counterstained with DAPI. Arrows, Epi; filled arrowheads, VE; empty arrowheads, ExE.

Development (2015) 142, 3675-3685 doi:10.1242/dev.125708

changed to any significant level (1.20-fold and 1.17-fold, respectively). *Bim*, which is not known as a p53 target, was unaffected (1.12-fold). No increase in the expression of *p21* and *Noxa* was observed in the proximal cell population.

p53-induced apoptosis is transcription independent

Since a fraction of p53 also non-transcriptionally controls the mitochondrial apoptotic pathway (Vaseva and Moll, 2009), we tested the requirement of transcription for DNA damage-induced apoptosis. E6.5 embryos were incubated in α-amanitin-containing serum for 30 min prior to 5 Gy irradiation and further cultured for 90 min in α-amanitin. The apoptotic phenotype was then analysed by Cl Casp-3 immunostaining. Treated embryos exhibited a lower average apoptotic index than controls incubated in the presence of DMSO (Fig. 4D), but the reduction was modest and not fully penetrant since only one out of four embryos presented an apoptotic index that was significantly reduced to 7%. Hence, control of apoptosis by p53 in the Epi is only partly dependent on transcription.

Thus, E6.5 Epi cells exhibit stronger DNA damage signalling. Their amplified local response at chromatin lesions at the level of 53BP1 recruitment correlates with a unique capacity to rapidly activate p53 upon DNA damage induction. Although the p53 transcriptional programme is rapidly activated in the Epi, transcription-independent properties of p53 are also involved in the apoptotic process.

p53 is activated in E5.5 Epi cells upon irradiation

Since the Epi cells are prone to undergo apoptosis upon low-dose irradiation and maintain this hypersensitivity as they enter the PrS, but lose it when they migrate away and differentiate, we hypothesized that the epigenetic environment peculiar to pluripotent cells might be responsible for the amplification of DNA damage signalling. This prompted us to analyse p53 behaviour in E5.5 embryos, which possess pluripotent Epi cells but are resistant to irradiation. Exposure of E5.5 embryos to 0.5 Gy induced the Epi-specific phosphorylation of p53 (Ser18) as early as 10 min after irradiation, as observed in E6.5 embryos (Fig. 4E). Hence, this particularly rapid activation of p53 seems to be a common feature of pluripotent Epi cells. Importantly, this result shows that p53 activation is essential but not sufficient to explain Epi-specific radiation-induced apoptosis at E6.5.

Epi cells are primed for apoptosis

We reasoned that if the DNA damage-induced apoptosis observed in the Epi is not dependent on transcription, then it must depend on a reservoir of constitutive pro-apoptotic effector proteins. A comparative analysis of transcripts coding for pro- and anti-apoptotic factors in E7.5 distal and proximal cell populations revealed that pro-apoptotic *Bim* and *Noxa* were more highly expressed in the Epi-containing cell population by 2-fold and 9-fold, respectively, whereas *Bak*, *Bax* and *Bid* were not affected (Fig. 5A, Fig. S5A,B). The anti-apoptotic factors *Bcl-xL* and *Mcl1* did not exhibit any differential expression. In addition, immunoblots of E7.5 distal and proximal cell populations showed equal expression of Bax but showed a 2-fold higher level of Bak and Bim in the distal cells (Fig. 5B, Fig. S5A-C). By contrast, Bcl-xL was downregulated 1.9-fold in this tissue. Unfortunately, no antibody was available to test for Noxa expression. Therefore, at E7.5 Epi cells express higher levels of the pro-apoptotic factors *Noxa* (at the RNA level), Bak (at the protein level) and Bim (at both RNA and protein levels), whereas the anti-apoptotic Bcl-xL is downregulated (at the protein level).

As these analyses were performed in E7.5 embryos, we used immunofluorescence to test the expression of Bak, Bim and Bcl-xL at E6.5. Interestingly, Bak staining was stronger in the Epi cells and largely colocalised with the Mito-ID mitochondrial marker (Fig. 5C). We also observed a striking difference in the intensity of Bim immunostaining, which was much weaker in the ExE and completely absent from the VE (Fig. 5D). Unlike Bak, the Bim signal was more diffuse and colocalised more rarely with Mito-ID dye, suggesting that Bim is involved both in mitochondrial and cytosolic complexes in Epi cells. Conversely, Bcl-xL showed stronger expression in the extra-embryonic tissues and was found both at the mitochondria and in the cytosol (Fig. 5E). In conclusion, these results suggest that the apoptotic threshold is lower in the Epi than in extra-embryonic cell types, which primes Epi cells to rapidly undergo apoptosis upon p53 activation.

Epi cytoplasmic priming is set between E5.5 and E6.5

Compared with E6.5 and E7.5, Bak, Bim and Bcl-xL showed different expression patterns at E5.5. Bak was detected at extremely low levels at E5.5, and thus did not demonstrate any enhanced expression in the Epi (Fig. 5F), whereas Bim was expressed evenly in the Epi and ExE (Fig. 5G) and Bcl-xL was detected at equal intensity in all cell types (Fig. 5H). This contrasts with the results obtained in E6.5 and E7.5 embryos and suggests that the resistance of E5.5 embryos to irradiation, in spite of p53 activation in the Epi, is due to the lack of a permissive apoptotic balance. Thus, the expression of pro- and anti-apoptotic factors is tightly controlled in the peri-gastrulation mouse Epi, allowing a remodelling of the apoptotic threshold between E5.5 and E6.5 via an increase in Bak and Bim expression and a decrease in Bcl-xL.

DISCUSSION

As they enter a phase of high proliferation, mouse Epi cells show a remarkable sensitivity to exogenous DNA damage, undergoing apoptosis at very low radiation dose. This protective mechanism, which operates in a sharply defined window of development, is expected to eliminate potentially dangerous mutation carriers before their clonal expansion. This hypersensitivity toward apoptosis relies on the convergence of several regulatory mechanisms. Indeed, we have shown that Epi cells exhibit an amplification of 53BP1 DNA damage signalling on the chromatin, leading to a strikingly rapid and specific activation of p53 in this tissue. In addition, after E5.5, Epi cells lower their apoptotic threshold by elevating the expression of pro-apoptotic Bak and Bim and downregulating Bcl-xL, which primes and sensitises cells to undergo apoptosis upon p53 activation (Fig. 6).

Hypersensitivity to radiation correlates with hyperproliferation in the Epi

Epi cells become hypersensitive as they enter a phase of intense expansion (Fig. S1A,B). Therefore, they may suffer from replicative stress, topological constraints of replication or replication/transcription conflicts (Helmrich et al., 2011; Postow et al., 2001). Part of the complexity of the DNA damage response derives from the important crosstalk with the replication machinery. Components of the DNA damage response pathway also play roles in replication or replication/transcription coupling, independently of DNA damage induction (Gamper et al., 2012; Olcina et al., 2013; Shechter et al., 2004; Turinetto et al., 2012). Hence, one could argue that the DNA damage response may be altered in Epi cells during this developmental window because of their high proliferation rate. Indeed, mitotic chromosomes are P-S/TQ positive in the Epi,

Development (2015) 142, 3675-3685 doi:10.1242/dev.125708

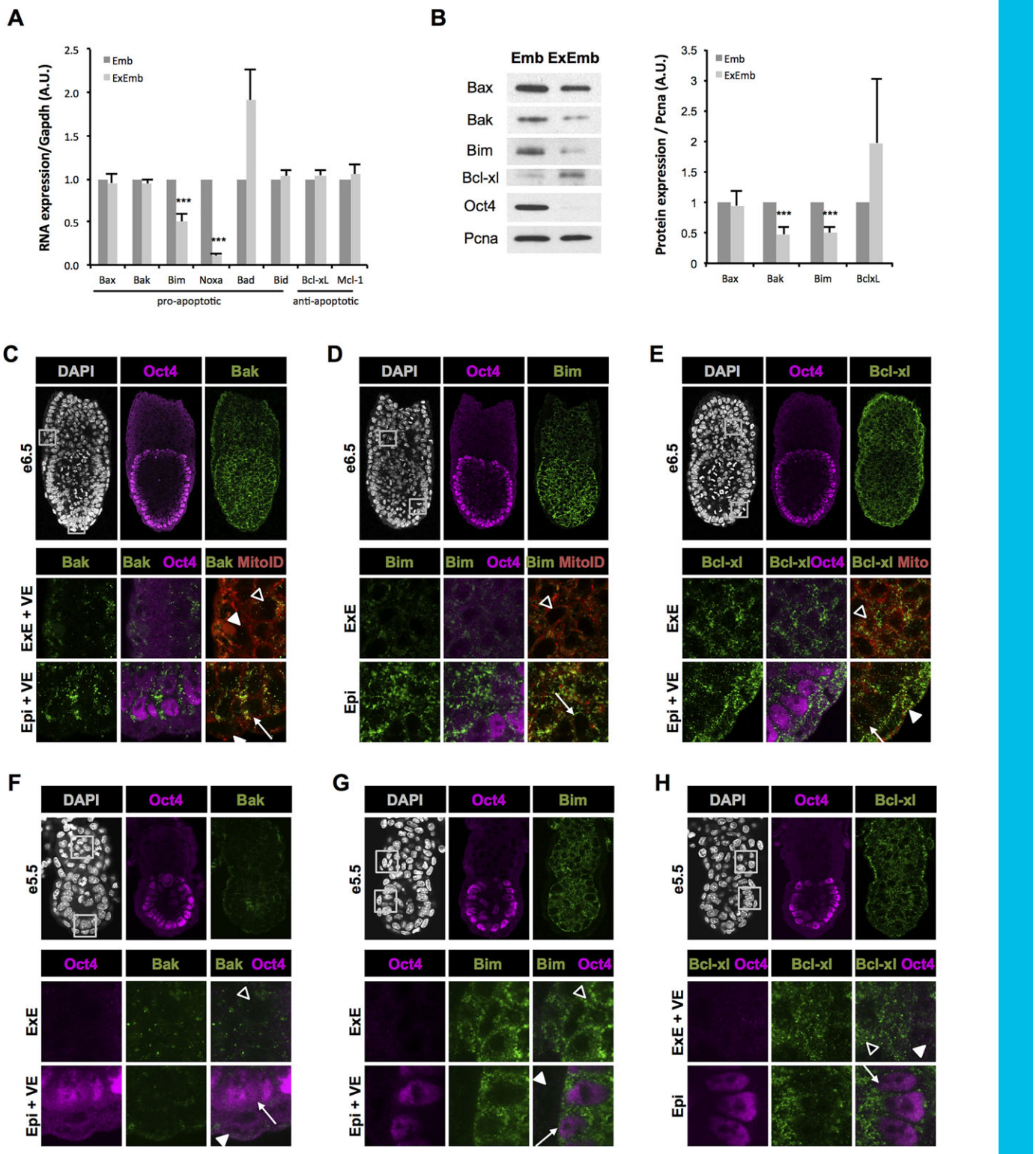

Fig. 5. Epi cells are primed for apoptosis. (A) qRT-PCR analysis of *Bax*, *Bak*, *Bim*, *Noxa*, *Bad*, *Bid*, *Bcl-xL* and *Mcl1* expression in E7.5 distal (Emb) and proximal (ExEmb) cell populations (n=3). (B) Representative immunoblot of Bax, Bak, Bim, Bcl-xL, Oct4 and Pcna in E7.5 distal and proximal cell populations. The plot presents the average of quantifications measured in three independent experiments; error bars indicate s.d. ***P<0.005, Student's t-test. (C-H) Representative immunostainings of Oct4 and Bak (C,F) (n=4), Oct4 and Bim (D,G) (n=5 at E6.5, n=4 at E5.5) and Oct4 and Bcl-xL (E,H) (n=4) in E6.5 (C-E) and E5.5 (F-H) embryos, counterstained with DAPI. Boxed regions are magnified beneath. Arrows, Epi; filled arrowheads, VE; empty arrowheads, ExE.

independently of exogenous stress induction (Fig. S3B), and Epi cells show notable levels of replicative stress (Fig. S1C,D). However, we showed that the ExE exhibited similar levels of stress without exhibiting hypersensitivity. Therefore, the replicative stress alone cannot justify the differential apoptotic behaviour of the Epi upon low-dose irradiation.

Development (2015) 142, 3675-3685 doi:10.1242/dev.125708

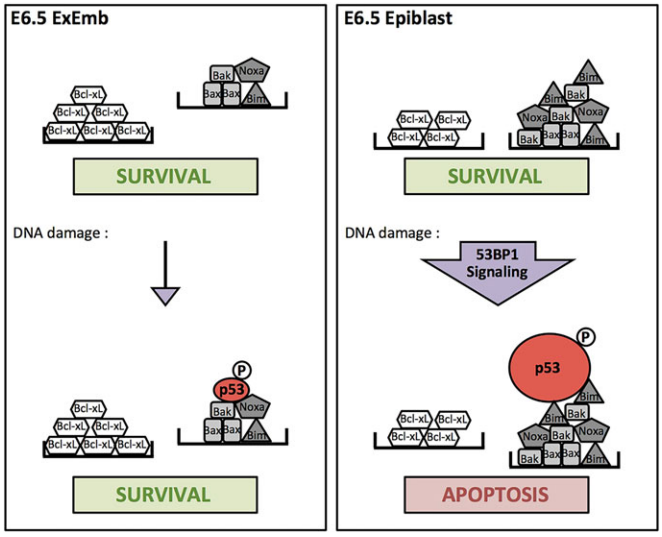

Fig. 6. Model of cellular determinants driving hypersensitivity of the Epi. The apoptotic threshold is depicted as a balance, the equilibrium of which is impacted by the ratio between pro- and anti-apoptotic factors. After E5.5, the pro-apoptotic factors Bak, Bim and Noxa (grey) are more abundant in the Epi than in extra-embryonic tissues (ExEmb), and anti-apoptotic Bcl-xL (white) is less expressed, priming the cells for apoptosis. Upon induction of DNA damage, increased signalling in Epi cells leads to rapid phosphorylation of p53. The activation of p53 provides an additional 'weight' that is sufficient to cross the apoptotic threshold and trigger apoptosis in the primed Epi cells.

Epi cells possess highly responsive chromatin

We found that Epi cells differ in their early DNA damage response, showing increased 53BP1 focal recruitment at the site of DNA breaks (Fig. 3D). Importantly, the measurement of similar amounts of γH2AX immunofluorescence in the Epi and extra-embryonic tissues rules out the possibility that radiation causes more damage in the Epi than in other cell types (Fig. 3B). Instead, pluripotent cells are often reported to possess loose, plastic and highly dynamic chromatin, which may facilitate rapid reorganisation and response to environmental cues. In fact, Murga and colleagues have shown that the relaxation of chromatin by depletion or inhibition of histone H1 in mouse ESCs triggers an amplified response to DNA damage (Murga et al., 2007). Differences in the epigenetic background between Epi, ExE and VE might interfere with 53BP1 recruitment and/or stability upon DNA damage.

The increased 53BP1 recruitment is of particular interest when considering the position of 53BP1 in the cascade of the DNA damage response. In addition to its function as a mediator of DNA damage signalling, 53BP1 is also an amplifier of the response, as it can interact directly with the upstream sensor Rad50 (a component of the MRN complex), generating a positive-feedback loop that allows spreading of the signalling along the broken chromatin and increased activation of Atm (Lee et al., 2010; Mochan et al., 2003). It is tempting to speculate that, as in mouse embryonic fibroblasts (Fernandez-Capetillo et al., 2002), 53BP1 is essential to promote Atm, Atr or DNA-PK activation in Epi cells upon low-dose radiation and amplifies a DNA damage signalling that might otherwise be insufficient to induce apoptosis. Thus, the specific focal recruitment of 53BP1 in Epi cells may sensitise them to low-dose irradiation. However, how this is achieved and how this affects Atm, Atr and DNA-PK remains to be elucidated.

Rapid activation of p53 controls apoptotic behaviour in the Epi

Following enhanced 53BP1 recruitment at double-stranded breaks, p53 is phosphorylated on Ser18 remarkably quickly in Epi cells: 10 min after 0.5 Gy irradiation versus 1 h in extra-embryonic tissues (Fig. 4A). To our knowledge, such rapid p53 activation is unique. Thus, we demonstrate a specific overall exacerbation of DNA damage signalling in Epi cells, both at the level of 53BP1 recruitment on the chromatin and at the level of p53 activation. These two phenomena are very likely functionally linked since 53BP1 is essential to support p53 activation by Atm (Panier and Boulton, 2014; Wang et al., 2002; Ward et al., 2003). We should emphasize, however, that alternative Atm-independent mechanisms might account for rapid p53 activation since *Atm*-null embryos were able to undergo apoptosis even more efficiently than wild type (Fig. 3C). In fact, Atr and DNA-PK kinases are also able to phosphorylate human P53 on Ser15 (Lees-Miller et al., 1992; Tibbetts et al., 1999). Accordingly, we found that p53 was equally activated in *Atm*-null and wild-type embryos after 0.5 Gy irradiation (Fig. S7).

In the Epi, p53 activation results in the induction of its transcriptional properties: *p21* and *Noxa* were upregulated as early as 1 h after 0.5 Gy irradiation (Fig. 4C). However, p53 function in the apoptotic process cannot exclusively depend on its transcriptional activity, since embryos incubated in α-amanitin were able to undergo apoptosis, albeit milder (Fig. 4D). Therefore, we conclude that p53 must control the mitochondrial apoptotic pathway primarily through a post-transcriptional mechanism, reinforced by the transcriptional induction of p53 targets. Indeed, increasing evidence suggests that the first wave of p53 action in apoptosis is exerted via direct interactions with proapoptotic Bax (Chipuk et al. 2004) and Bak (Leu et al., 2004) or antiapoptotic Bcl2 (Tomita et al., 2006) and Bcl-xL (Mihara et al., 2003). Such a strategy for p53 action has been reported in human ESCs (Liu et al., 2013).

Although P-p53 immunoreactivity was reproducibly observed with a significant delay in the ExE compared with the Epi, 1 h after irradiation it had reached a similar level of intensity in both tissues (Fig. 4A). But even 2 h after irradiation, p53 activation in the ExE was not associated with apoptosis (Fig. 2A). Thus, exposure to p53 Ser18 phosphorylation for similar periods of time (1 h) in the Epi and in the adjacent ExE leads to two different cellular outcomes. Similarly, the rapid activation of p53 in the Epi of E5.5 embryos was not followed by an apoptotic behaviour (Fig. 4E). This emphasizes the complexity of p53 activity, which is regulated via numerous post-translational modifications (Carvajal and Manfredi, 2013; Vousden and Prives, 2009). In E6.5 Epi cells, p53 may carry additional modifications or meet different interacting partners, which would explain its differential effect on apoptosis. Alternatively, this result might suggest that p53 activation is necessary but not sufficient for apoptosis induction and confirms the idea that cytoplasmic determinants are also crucial for p53-induced apoptosis (Fig. 4D) (Kracikova et al., 2013).

Elevated expression of Noxa, Bim and Bak lowers the apoptotic threshold of Epi cells

The 9-fold higher expression of *Noxa* mRNA in the Epi-containing distal cell population compared with the proximal extra-embryonic annexes (Fig. 5A) agrees with the hypothesis that Epi cells require a permissive cytoplasmic context for p53-dependent induction of apoptosis. Unfortunately, no antibody was available to test the levels of Noxa protein expression. Interestingly, Gutekunst and colleagues reported an Oct4-mediated Noxa upregulation in testicular germ cell tumours, rendering them hypersensitive to cisplatin treatment (Gutekunst et al., 2013).

Development (2015) 142, 3675-3685 doi:10.1242/dev.125708

In addition, we showed that Bak and Bim proteins are more abundant in the Epi, whereas Bcl-xL is more abundant in the ExE and VE (Fig. 5B-E). This suggests that Epi cells have a low apoptotic threshold, which must sensitise them to apoptosis. It is noteworthy that the timing of the cytoplasmic priming of the Epi cells correlates with the acquisition of hypersensitivity to radiation (Fig. 5F-H).

Although we found that Bax is highly expressed in the embryo (Fig. 5A,B), we were not able to detect its active form in the absence of irradiation (Fig. 1C), in contrast to what has been reported in human ESCs (Dumitru et al., 2012). On the other hand, we did not detect any increase in *Bim* mRNA after exposure to ionizing radiation (Fig. 4C), in contrast to what was suggested by a previous study on mouse embryos (Pernaute et al., 2014). These discrepancies between *in vitro* and *in vivo* assays underline the multiplicity of mechanisms by which cells can opt in or out of survival/death control.

In conclusion, we show that the hypersensitivity of Epi cells relies on the convergence of (1) an amplified DNA damage response and p53 signalling and (2) a high cytoplasmic priming toward apoptosis. It is noteworthy that this low apoptotic threshold might play an equally important role in other types of stresses, such as those associated with a lack of nutrients or growth factors, or Myc-driven cell competition (Clavería et al., 2013; Sancho et al., 2013). Thus, because of the high level of vigilance of Epi cells at the E5.5-6.5 transition, it is not surprising that so many mouse mutants are lethal at this specific stage, a representative example being *Mdm2*$^{-/-}$ (Jones et al., 1995): the depletion of this p53 inhibitor induces apoptosis after E5.5 in Epi cells, which we now show concomitantly express consistent levels of p53 and are very close to crossing the apoptotic threshold.

Future research should aim at unravelling the molecular link that couples the increase in proliferative rate, the commitment to differentiation and the tight regulation of pro-apoptotic balance at the peri-gastrulation stage in the Epi.

MATERIALS AND METHODS

Embryo recovery and treatment

C57BL/6 embryos were extracted by standard procedures into M2 medium (Sigma-Aldrich) and cultured in ESC-tested fetal calf serum at 37°C, 5% CO_2. X-ray irradiation was performed in a Faxitron RX-650 device. For α-amanitin treatment, embryos were incubated in 50 µg/ml α-amanitin-containing serum (Sigma-Aldrich) for 30 min prior to irradiation and further cultured for 90 min in α-amanitin. For *p53* and *Atm* genotyping, embryos were lysed in a buffer containing 10 mM Tris HCl pH 8.4, 50 mM KCl, 2 mM $MgCl_2$, 0.45% NP-40, 0.45% Tween 20 and 3 µg/µl proteinase K. Primers are detailed in Table S1. Animal experiments were carried out following the regulations of Italian law, upon authorisation 109/2011-PR of the Italian Ministry of Health.

Wholemount immunofluorescence

Embryos were fixed in 4% paraformaldehyde for 2 h at room temperature (RT) and washed in PBS/0.1% Tween 20. After permeabilisation in PBS/1% Triton X-100 for 30 min at RT, embryos were blocked in PBS/0.1% Triton X-100/3% bovine serum albumin for 2 h at RT. They were then incubated with primary antibodies diluted in blocking buffer for 1 h at RT. Primary antibodies are detailed in the supplementary Materials and Methods. Embryos were washed and incubated with secondary antibodies diluted in PBS/0.1% Triton X-100: Cy3-conjugated donkey anti-rabbit (Jackson Labs, 711-165-152; 1:400) and Alexa Fluor 647-conjugated donkey anti-goat (Invitrogen, A-21447; 1:400). In experiments using the Mito-ID Red dye, Alexa Fluor 488-conjugated donkey anti-rabbit secondary antibody (Invitrogen, A-21206; 1:400) was used. After washes, embryos were counterstained with DAPI (0.5 µg/ml) and eventually with Mito-ID Red (Enzo Life Sciences, 1/2000). For active Bax immunostaining, biotin-coupled primary antibody was detected with FITC-coupled streptavidin (Sigma-Aldrich, 100 µg/ml). Confocal images were captured using a Leica TCS SP2 microscope. For quantification of immunofluorescence in γH2AX and 53BP1 foci, *z*-stack images were acquired every 0.5 µm. Using Fiji software, images were cropped at the border of the cells of interest on every confocal section and a maximum *z*-projection was performed. The amount of fluorescence per cell was calculated as the sum of (area/foci×mean intensity/foci) for each focus analysed by Fiji.

RNA expression analysis

Embryos were dissected at the embryonic/extra-embryonic border. For each condition, a minimum of seven isolated embryonic or extra-embryonic poles were pooled and RNAs were extracted using the RNeasy Kit (Qiagen). The reverse transcription was performed on 250 ng RNA with Superscript III (Invitrogen). Samples, incubated with primers and LightCycler 480 SYBR Green I Master (Roche), were run in duplicate on a LightCycler 480 (Roche) machine. The results were normalised to *Gapdh* gene expression. Primers are detailed in Table S1.

Immunoblotting

Embryonic and extra-embryonic poles were pooled and protein extracts were obtained by lysis in Laemmli buffer in the presence of protease inhibitors. Primary antibodies are detailed in the supplementary Materials and Methods. Protein levels were quantified in ImageJ (NIH) and normalised to Pcna.

Acknowledgements

We thank Dr Shankar Srinivas for sharing expertise on E5.5 embryo manipulation; Dr Marek Adamowicz for helpful scientific discussions; and Dr Luis Fernandez-Diaz, Dr Divya Purushothaman and Dr Arsen Petrovic for comments on the manuscript.

Competing interests

The authors declare no competing or financial interests.

Author contributions

Experiments were designed and performed by A.L. under the supervision of F.B. The manuscript was prepared by A.L. and F.B.

Funding

A.L. was supported by a Fondazione Umberto Veronesi fellowship. F.B. was supported by the Italian Association for Cancer Research [grant no. BM0805], Cariplo Foundation and Italian Ministry of Health.

Supplementary information

Supplementary information available online at
http://dev.biologists.org/lookup/suppl/doi:10.1242/dev.125708/-/DC1

References

Anderson, L., Henderson, C. and Adachi, Y. (2001). Phosphorylation and rapid relocalization of 53BP1 to nuclear foci upon DNA damage. *Mol. Cell. Biol.* **21**, 1719-1729.

Blanpain, C., Mohrin, M., Sotiropoulou, P. A. and Passegué, E. (2011). DNA-damage response in tissue-specific and cancer stem cells. *Cell Stem Cell* **8**, 16-29.

Brown, E. J. and Baltimore, D. (2000). ATR disruption leads to chromosomal fragmentation and early embryonic lethality. *Genes Dev.* **14**, 397-402.

Callén, E., Jankovic, M., Wong, N., Zha, S., Chen, H.-T., Difilippantonio, S., Di Virgilio, M., Heidkamp, G., Alt, F. W., Nussenzweig, A. et al. (2009). Essential role for DNA-PKcs in DNA double-strand break repair and apoptosis in ATM-deficient lymphocytes. *Mol. Cell* **34**, 285-297.

Carvajal, L. A. and Manfredi, J. J. (2013). Another fork in the road—life or death decisions by the tumour suppressor p53. *EMBO Rep.* **14**, 414-421.

Chipuk, J. E., Kuwana, T., Bouchier-Hayes, L., Droin, N. M., Newmeyer, D. D., Schuler, M. and Green, D. R. (2004). Direct activation of Bax by p53 mediates mitochondrial membrane permeabilization and apoptosis. *Science* **303**, 1010-1014.

Clavería, C., Giovinazzo, G., Sierra, R. and Torres, M. (2013). Myc-driven endogenous cell competition in the early mammalian embryo. *Nature* **500**, 39-44.

Dobles, M., Liberal, V., Scott, M. L., Benezra, R. and Sorger, P. K. (2000). Chromosome missegregation and apoptosis in mice lacking the mitotic checkpoint protein Mad2. *Cell* **101**, 635-645.

Development (2015) 142, 3675-3685 doi:10.1242/dev.125708

Dumaz, N., Milne, D. M. and Meek, D. W. (1999). Protein kinase CK1 is a p53-threonine 18 kinase which requires prior phosphorylation of serine 15. *FEBS Lett.* **463**, 312-316.

Dumitru, R., Gama, V., Fagan, B. M., Bower, J. J., Swahari, V., Pevny, L. H. and Deshmukh, M. (2012). Human embryonic stem cells have constitutively active Bax at the Golgi and are primed to undergo rapid apoptosis. *Mol. Cell* **46**, 573-583.

Fernandez-Capetillo, O., Chen, H.-T., Celeste, A., Ward, I., Romanienko, P. J., Morales, J. C., Naka, K., Xia, Z., Camerini-Otero, R. D., Motoyama, N. et al. (2002). DNA damage-induced G2–M checkpoint activation by histone H2AX and 53BP1. *Nat. Cell Biol.* **4**, 993-997.

Gamper, A. M., Choi, S., Matsumoto, Y., Banerjee, D., Tomkinson, A. E. and Bakkenist, C. J. (2012). ATM protein physically and functionally interacts with proliferating cell nuclear antigen to regulate DNA synthesis. *J. Biol. Chem.* **287**, 12445-12454.

Greaves, M. F. and Wiemels, J. (2003). Origins of chromosome translocations in childhood leukaemia. *Nat. Rev. Cancer* **3**, 639-649.

Gurley, K. E. and Kemp, C. J. (2001). Synthetic lethality between mutation in Atm and DNA-PKcs during murine embryogenesis. *Curr. Biol.* **11**, 191-194.

Gutekunst, M., Mueller, T., Weilbacher, A., Dengler, M. A., Bedke, J., Kruck, S., Oren, M., Aulitzky, W. E. and van der Kuip, H. (2013). Cisplatin hypersensitivity of testicular germ cell tumors is determined by high constitutive Noxa levels mediated by Oct-4. *Cancer Res.* **73**, 1460-1469.

Hafner, C., Toll, A. and Real, F. X. (2011). HRAS mutation mosaicism causing urothelial cancer and epidermal nevus. *N. Engl. J. Med.* **365**, 1940-1942.

Hakem, R., de la Pompa, J. L., Sirard, C., Mo, R., Woo, M., Hakem, A., Wakeham, A., Potter, J., Reitmair, A., Billia, F. et al. (1996). The tumor suppressor gene Brca1 is required for embryonic cellular proliferation in the mouse. *Cell* **85**, 1009-1023.

Helmrich, A., Ballarino, M. and Tora, L. (2011). Collisions between replication and transcription complexes cause common fragile site instability at the longest human genes. *Mol. Cell* **44**, 966-977.

Hendzel, M. J., Wei, Y., Mancini, M. A., Van Hooser, A., Ranalli, T., Brinkley, B. R., Bazett-Jones, D. P. and Allis, C. D. (1997). Mitosis-specific phosphorylation of histone H3 initiates primarily within pericentromeric heterochromatin during G2 and spreads in an ordered fashion coincident with mitotic chromosome condensation. *Chromosoma* **106**, 348-360.

Herrmann, B. G., Labeit, S., Poustka, A., King, T. R. and Lehrach, H. (1990). Cloning of the T gene required in mesoderm formation in the mouse. *Nature* **343**, 617-622.

Heyer, B. S., MacAuley, A., Behrendtsen, O. and Werb, Z. (2000). Hypersensitivity to DNA damage leads to increased apoptosis during early mouse development. *Genes Dev.* **14**, 2072-2084.

Hsu, Y.-T., Wolter, K. G. and Youle, R. J. (1997). Cytosol-to-membrane redistribution of Bax and Bcl-XL during apoptosis. *Proc. Natl. Acad. Sci. USA* **94**, 3668-3672.

Jeon, Y., Ko, E., Lee, K. Y., Ko, M. J., Park, S. Y., Kang, J., Jeon, C. H., Lee, H. and Hwang, D. S. (2011). TopBP1 deficiency causes an early embryonic lethality and induces cellular senescence in primary cells. *J. Biol. Chem.* **286**, 5414-5422.

Jones, S. N., Roe, A. E., Donehower, L. A. and Bradley, A. (1995). Rescue of embryonic lethality in Mdm2-deficient mice by absence of p53. *Nature* **378**, 206-208.

Kalitsis, P., Earle, E., Fowler, K. J. and Andy Choo, K. H. (2000). Bub3 gene disruption in mice reveals essential mitotic spindle checkpoint function during early embryogenesis. *Genes Dev.* **14**, 2277-2282.

Kim, S.-T., Lim, D.-S., Canman, C. E. and Kastan, M. B. (1999). Substrate specificities and identification of putative substrates of ATM kinase family members. *J. Biol. Chem.* **274**, 37538-37543.

Kracikova, M., Akiri, G., George, A., Sachidanandam, R. and Aaronson, S. A. (2013). A threshold mechanism mediates p53 cell fate decision between growth arrest and apoptosis. *Cell Death Differ.* **20**, 576-588.

Lee, J.-H., Goodarzi, A. A., Jeggo, P. A. and Paull, T. T. (2010). 53BP1 promotes ATM activity through direct interactions with the MRN complex. *EMBO J.* **29**, 574-585.

Lees-Miller, S. P., Sakaguchi, K., Ullrich, S. J., Appella, E. and Anderson, C. W. (1992). Human DNA-activated protein kinase phosphorylates serines 15 and 37 in the amino-terminal transactivation domain of human p53. *Mol. Cell. Biol.* **12**, 5041-5049.

Leu, J. I.-J., Dumont, P., Hafey, M., Murphy, M. E. and George, D. L. (2004). Mitochondrial p53 activates Bak and causes disruption of a Bak–Mcl1 complex. *Nat. Cell Biol.* **6**, 443-450.

Liu, J. C., Guan, X., Ryan, J. A., Rivera, A. G., Mock, C., Agarwal, V., Letai, A., Lerou, P. H. and Lahav, G. (2013). High mitochondrial priming sensitizes hESCs to DNA-damage-induced apoptosis. *Cell Stem Cell* **13**, 483-491.

Marshall, G. M., Carter, D. R., Cheung, B. B., Liu, T., Mateos, M. K., Meyerowitz, J. G. and Weiss, W. A. (2014). The prenatal origins of cancer. *Nat. Rev. Cancer* **14**, 277-289.

Mihara, M., Erster, S., Zaika, A., Petrenko, O., Chittenden, T., Pancoska, P. and Moll, U. M. (2003). p53 has a direct apoptogenic role at the mitochondria. *Mol. Cell* **11**, 577-590.

Mochan, T. A., Venere, M., DiTullio, R. A., Jr and Halazonetis, T. D. (2003). 53BP1 and NFBD1/MDC1-Nbs1 function in parallel interacting pathways activating ataxia-telangiectasia mutated (ATM) in response to DNA damage. *Cancer Res.* **63**, 8586-8591.

Mori, H., Colman, S. M., Xiao, Z., Ford, A. M., Healy, L. E., Donaldson, C., Hows, J. M., Navarrete, C. and Greaves, M. (2002). Chromosome translocations and covert leukemic clones are generated during normal fetal development. *Proc. Natl. Acad. Sci. USA* **99**, 8242-8247.

Murga, M., Jaco, I., Fan, Y., Soria, R., Martinez-Pastor, B., Cuadrado, M., Yang, S.-M., Blasco, M. A., Skoultchi, A. I. and Fernandez-Capetillo, O. (2007). Global chromatin compaction limits the strength of the DNA damage response. *J. Cell Biol.* **178**, 1101-1108.

Olcina, M. M., Foskolou, I. P., Anbalagan, S., Senra, J. M., Pires, I. M., Jiang, Y., Ryan, A. J. and Hammond, E. M. (2013). Replication stress and chromatin context link ATM activation to a role in DNA replication. *Mol. Cell* **52**, 758-766.

Palmieri, S. L., Peter, W., Hess, H. and Schöler, H. R. (1994). Oct-4 transcription factor is differentially expressed in the mouse embryo during establishment of the first two extraembryonic cell lineages involved in implantation. *Dev. Biol.* **166**, 259-267.

Panier, S. and Boulton, S. J. (2014). Double-strand break repair: 53BP1 comes into focus. *Nat. Rev. Mol. Cell Biol.* **15**, 7-18.

Pernaute, B., Spruce, T., Smith, K. M., Sánchez-Nieto, J. M., Manzanares, M., Cobb, B. and Rodríguez, T. A. (2014). MicroRNAs control the apoptotic threshold in primed pluripotent stem cells through regulation of BIM. *Genes Dev.* **28**, 1873-1878.

Postow, L., Crisona, N. J., Peter, B. J., Hardy, C. D. and Cozzarelli, N. R. (2001). Topological challenges to DNA replication: conformations at the fork. *Proc. Natl. Acad. Sci. USA* **98**, 8219-8226.

Saito, S., Goodarzi, A. A., Higashimoto, Y., Noda, Y., Lees-Miller, S. P., Appella, E. and Anderson, C. W. (2002). ATM mediates phosphorylation at multiple p53 sites, including Ser46, in response to ionizing radiation. *J. Biol. Chem.* **277**, 12491-12494.

Sancho, M., Di-Gregorio, A., George, N., Pozzi, S., Sánchez, J. M., Pernaute, B. and Rodríguez, T. A. (2013). Competitive interactions eliminate unfit embryonic stem cells at the onset of differentiation. *Dev. Cell* **26**, 19-30.

Seo, J., Kim, S. C., Lee, H.-S., Kim, J. K., Shon, H. J., Salleh, N. L. M., Desai, K. V., Lee, J. H., Kang, E.-S., Kim, J. S. et al. (2012). Genome-wide profiles of H2AX and gamma-H2AX differentiate endogenous and exogenous DNA damage hotspots in human cells. *Nucleic Acids Res.* **40**, 5965-5974.

Shechter, D., Costanzo, V. and Gautier, J. (2004). ATR and ATM regulate the timing of DNA replication origin firing. *Nat. Cell Biol.* **6**, 648-655.

Siliciano, J. D., Canman, C. E., Taya, Y., Sakaguchi, K., Appella, E. and Kastan, M. B. (1997). DNA damage induces phosphorylation of the amino terminus of p53. *Genes Dev.* **11**, 3471-3481.

Snow, M. H. L. (1977). Gastrulation in the mouse: growth and regionalization of the epiblast. *J. Embryol. Exp. Morphol.* **42**, 293-303.

Solter, D., Škreb, N. and Damjanov, I. (1971). Cell cycle analysis in the mouse EGG-cylinder. *Exp. Cell Res.* **64**, 331-334.

Stuckey, D. W., Clements, M., Di-Gregorio, A., Senner, C. E., Le Tissier, P., Srinivas, S. and Rodriguez, T. A. (2011). Coordination of cell proliferation and anterior-posterior axis establishment in the mouse embryo. *Development* **138**, 1521-1530.

Takaoka, K. and Hamada, H. (2012). Cell fate decisions and axis determination in the early mouse embryo. *Development* **139**, 3-14.

Tibbetts, R. S., Brumbaugh, K. M., Williams, J. M., Sarkaria, J. N., Cliby, W. A., Shieh, S.-Y., Taya, Y., Prives, C. and Abraham, R. T. (1999). A role for ATR in the DNA damage-induced phosphorylation of p53. *Genes Dev.* **13**, 152-157.

Tomita, Y., Marchenko, N., Erster, S., Nemajerova, A., Dehner, A., Klein, C., Pan, H., Kessler, H., Pancoska, P. and Moll, U. M. (2006). WT p53, but not tumor-derived mutants, bind to Bcl2 via the DNA binding domain and induce mitochondrial permeabilization. *J. Biol. Chem.* **281**, 8600-8606.

Turinetto, V., Orlando, L., Sanchez-Ripoll, Y., Kumpfmueller, B., Storm, M. P., Porcedda, P., Minieri, V., Saviozzi, S., Accomasso, L., Cibrario Rocchietti, E. et al. (2012). High basal gammaH2AX levels sustain self-renewal of mouse embryonic and induced pluripotent stem cells. *Stem Cells* **30**, 1414-1423.

Vaseva, A. V. and Moll, U. M. (2009). The mitochondrial p53 pathway. *Biochim. Biophys. Acta* **1787**, 414-420.

Vousden, K. H. and Prives, C. (2009). Blinded by the light: the growing complexity of p53. *Cell* **137**, 413-431.

Wang, B., Matsuoka, S., Carpenter, P. B. and Elledge, S. J. (2002). 53BP1, a mediator of the DNA damage checkpoint. *Science* **298**, 1435-1438.

Ward, I. M. and Chen, J. (2001). Histone H2AX is phosphorylated in an ATR-dependent manner in response to replicational stress. *J. Biol. Chem.* **276**, 47759-47762.

Ward, I. M., Minn, K., van Deursen, J. and Chen, J. (2003). p53 Binding protein 53BP1 is required for DNA damage responses and tumor suppression in mice. *Mol. Cell. Biol.* **23**, 2556-2563.

Williamson, C. T., Muzik, H., Turhan, A. G., Zamo, A., O'Connor, M. J., Bebb, D. G. and Lees-Miller, S. P. (2010). ATM deficiency sensitizes mantle cell lymphoma cells to poly(ADP-ribose) polymerase-1 inhibitors. *Mol. Cancer Ther.* **9**, 347-357.

Zeman, M. K. and Cimprich, K. A. (2014). Causes and consequences of replication stress. *Nat. Cell Biol.* **16**, 2-9.